INTERNATIONAL JOURNAL FOR NUMERICAL METHODS IN FLUIDS
Int. J. Numer. Meth. Fluids 2006; **50**:255–261
Published online 17 November 2005 in Wiley InterScience (www.interscience.wiley.com). DOI: 10.1002/fld.1130

Droplets on patterned substrates: Water off a beetle's back‡

A. Dupuis*,† and J. M. Yeomans

The Rudolf Peierls Centre for Theoretical Physics, University of Oxford, 1 Keble Road, Oxford OX1 3NP, U.K.

SUMMARY

We present a lattice Boltzmann model to describe the spreading of droplets on chemically and topologically patterned substrates. As an example, we consider the process by which a Namibian beetle captures water on its back which is hydrophobic but covered by peaks with hydrophilic tops. Copyright © 2005 John Wiley & Sons, Ltd.

KEY WORDS: lattice Boltzmann model; wetting; beetle; patterned substrate

1. INTRODUCTION

A droplet in contact with a substrate will try to spread to an equilibrium shape determined by the balance of surface tensions. This process is affected by the presence of surface inhomogeneity which may pin the drop, change its equilibrium shape and alter its spreading dynamics. This has usually been viewed as a nuisance in experiments and applications. However, with the advent of microfabrication techniques, it is becoming possible to harness controlled surface topologies to explore new physical phenomena.

A nice example is the way certain beetles living in the Namibian desert collect drinking water on their backs from a fog-laden wind [1]. Large water droplets form by virtue of the insect's bumpy surface, which consists of alternating hydrophobic and hydrophilic regions. The size of the drops then allows them to move against the wind into the beetle's mouth.

The aim of this paper is to present a lattice Boltzmann algorithm which can be used to investigate the behaviour of droplets on patterned substrates. Lattice Boltzmann is a particularly appropriate approach in that it solves the Navier–Stokes equations but also inputs the thermodynamic information, such as surface tensions, needed to describe the behaviour of droplets.

*Correspondence to: A. Dupuis, The Rudolf Peierls Centre for Theoretical Physics, University of Oxford, 1 Keble Road, Oxford OX1 3NP, U.K.
†E-mail: dupuis@thphys.ox.ac.uk
‡This was originally submitted as part of the IFCD SPECIAL ISSUE.

Contract/grant sponsor: EC IMAGE-IN; contract/grant number: GR1D-CT-2002-00663

Received 27 April 2004
Revised 17 September 2004
Accepted 16 September 2005

Moreover its natural length scale, for fluids such as water, is of order microns where much of the exciting new physics is expected to appear. The method has already shown its capability in dealing with spreading on surfaces with chemical [2] and topological patterning [3].

In Section 2 we summarize the algorithm and describe the new thermodynamic and velocity boundary conditions needed to treat surfaces with topological patterning. In Section 3 we present results reproducing the way in which a beetle can capture water from a surrounding fog.

2. THE MESOSCOPIC MODEL

We consider a liquid–gas system of density $n(\mathbf{r})$ and volume V. The surface of the substrate is denoted by S. The equilibrium properties are described by the free energy

$$\Psi = \int_V \left(\psi_b(n) + \frac{\kappa}{2} (\partial_\alpha n)^2 \right) \mathrm{d}V + \int_S \psi_c(n)\, \mathrm{d}S \tag{1}$$

$\psi_b(n)$ is the free energy in the bulk. We choose a Van der Waals form

$$\psi_b(n) = p_c(v_n + 1)^2(v_n^2 - 2v_n + 3 - 2\beta\tau_w) \tag{2}$$

where $v_n = (n - n_c)/n_c$, $\tau_w = (T_c - T)/T_c$ and $p_c = \frac{1}{8}$, $n_c = \frac{7}{2}$ and $T_c = \frac{4}{7}$ are the critical pressure, density and temperature, respectively, and β is a constant typically equal to 0.1. The bulk pressure

$$p_b = p_c(v_n + 1)^2(3v_n^2 - 2v_n + 1 - 2\beta\tau_w) \tag{3}$$

The derivative term in Equation (1) models the free energy associated with an interface. κ is related to the surface tension. $\psi_c(n_s) = \phi_0 - \phi_1 n_s + \cdots$ is the Cahn surface free energy [4] which controls the wetting properties of the fluid.

The lattice Boltzmann algorithm solves the Navier–Stokes equations for this system. Because interfaces appear naturally within the model it is particularly well suited to looking at the behaviour of moving drops.

2.1. The lattice Boltzmann algorithm

The lattice Boltzmann approach follows the evolution of partial distribution functions f_i on a regular, d-dimensional lattice formed of sites $\mathbf{r}$. The label i denotes velocity directions and runs between 0 and z. $DdQz + 1$ is a standard lattice topology classification. The $D3Q15$ lattice we use here has the following velocity vectors $\mathbf{v}_i$: $(0,0,0)$, $(\pm1,\pm1,\pm1)$, $(\pm1,0,0)$, $(0,\pm1,0)$, $(0,0,\pm1)$ in lattice units.

The lattice Boltzmann dynamics are given by

$$f_i(\mathbf{r} + \Delta t \mathbf{v}_i, t + \Delta t) = f_i(\mathbf{r}, t) + \frac{1}{\tau}(f_i^{\mathrm{eq}}(\mathbf{r}, t) - f_i(\mathbf{r}, t)) + n v_{i\alpha} F_\alpha \tag{4}$$

where Δt is the time step of the simulation, τ the relaxation time, $\mathbf{F}$ is a body force (Einstein notation is understood for α) and f_i^{eq} the equilibrium distribution function which is a function

of the density $n = \sum_{i=0}^{z} f_i$ and the fluid velocity $\mathbf{u}$, defined through the relation

$$n\mathbf{u} = \sum_{i=0}^{z} f_i \mathbf{v}_i \tag{5}$$

The relaxation time tunes the kinematic viscosity as [5]

$$v = \frac{\Delta \mathbf{r}^2}{\Delta t} \frac{L_4}{L_2} \left(\tau - \frac{1}{2} \right) \tag{6}$$

where $\Delta \mathbf{r}$ is the lattice spacing and L_2 and L_4 are coefficients related to the topology of the lattice. These are equal to 3 and 1, respectively, when one considers a $D3Q15$ lattice.

It can be shown [6] that Equation (4) reproduces the Navier–Stokes equations of a non-ideal gas if the local equilibrium functions are chosen as

$$\begin{aligned} f_i^{\mathrm{eq}} &= A_\sigma + B_\sigma u_\alpha v_{i\alpha} + C_\sigma \mathbf{u}^2 + D_\sigma u_\alpha u_\beta v_{i\alpha} v_{i\beta} + G_{\sigma\alpha\beta} v_{i\alpha} v_{i\beta}, \quad i > 0 \\ f_0^{\mathrm{eq}} &= n - \sum_{i=1}^{z} f_i^{\mathrm{eq}} \end{aligned} \tag{7}$$

where Einstein notation is understood for the Cartesian labels α and β (i.e. $v_{i\alpha} u_\alpha = \sum_\alpha v_{i\alpha} u_\alpha$) and where σ labels velocities of different magnitude. A possible choice of the coefficients is [7]

$$\begin{aligned} A_\sigma &= \frac{w_\sigma}{c^2} \left(p_{\mathrm{b}} - \frac{\kappa}{2} (\partial_\alpha n)^2 - \kappa n \partial_{\alpha\alpha} n + v u_\alpha \partial_\alpha n \right) \\ B_\sigma &= \frac{w_\sigma n}{c^2}, \quad C_\sigma = -\frac{w_\sigma n}{2c^2}, \quad D_\sigma = \frac{3 w_\sigma n}{2c^4} \\ G_{1\gamma\gamma} &= \frac{1}{2c^4} (\kappa (\partial_\gamma n)^2 + 2 v u_\gamma \partial_\gamma n), \quad G_{2\gamma\gamma} = 0 \\ G_{2\gamma\delta} &= \frac{1}{16 c^4} (\kappa (\partial_\gamma n)(\partial_\delta n) + v (u_\gamma \partial_\delta n + u_\delta \partial_\gamma n)) \end{aligned} \tag{8}$$

where $w_1 = \frac{1}{3}$, $w_2 = \frac{1}{24}$ and $c = \Delta \mathbf{r} / \Delta t$.

2.2. Wetting boundary conditions

The major challenge in dealing with patterned substrates is to handle the boundary conditions correctly. We consider first wetting boundary conditions which control the value of the density derivative and hence the contact angle. For flat substrates a boundary condition can be established by minimizing the free energy (1) [4]

$$\hat{\mathbf{s}} \cdot \nabla n = -\frac{\phi_1}{\kappa} \tag{9}$$

where $\hat{\mathbf{s}}$ is the unit vector normal to the substrate. It is possible to obtain an expression relating ϕ_1 to the contact angle θ as [8]

$$\phi_1 = 2\beta\tau_w \sqrt{2 p_{\mathrm{c}} \kappa}\, \mathrm{sign} \left(\frac{\pi}{2} - \theta \right) \sqrt{\cos\frac{\alpha}{3} \left(1 - \cos\frac{\alpha}{3} \right)} \tag{10}$$

where $\alpha = \cos^{-1}(\sin^2 \theta)$ and the function sign returns the sign of its argument.

Equation (9) is used to constrain the density derivative for sites on a flat part of the substrate. However, no such exact results are available for sites at edges or corners. We work on the principle that the wetting angle at such sites should be constrained as little as possible so that, in the limit of an increasingly fine mesh, it is determined by the contact angle of the neighbouring flat surfaces.

For edges (labels 9–12 in Figure 1) and corners (labels 1–4) at the top of the post each site has 6 neighbours on the computational mesh. Therefore, these sites can be treated as bulk sites.

At bottom edges where the post abuts the surface (labels 13–16 in Figure 1) density derivatives in the two directions normal to the surface (e.g. x and z for sites labelled 13) are calculated using

$$\partial_z n = \partial_{x/y} n = -\frac{1}{\sqrt{2}} \frac{\phi_1}{\kappa} \tag{11}$$

where the middle term constrains the density derivative in the appropriate direction x or y.

At bottom corners where the post joins the surface (labels 5–8 in Figure 1) density derivatives in both the x and y directions are known. Therefore, these sites are treated as planar sites.

In a hydrodynamic description of wetting contact line slip must be introduced in some way. As with other phase field models slip appears naturally within the lattice Boltzmann framework [9]. The mechanism responsible for the slip is described in some detail in Reference [8].

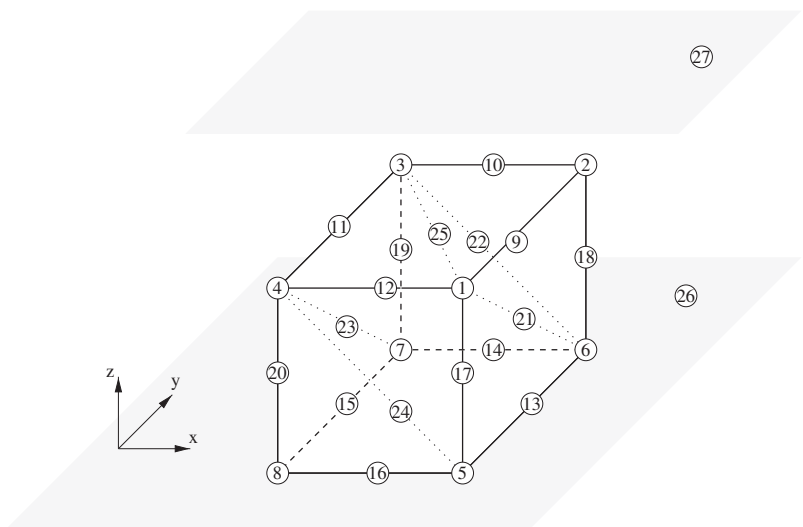

Figure 1. Sketch of a post on a substrate. Encircled numbers label sites in different topological positions. Labels 26 and 27 denote sites on the bottom ($z = z_{\min}$) and the top ($z = z_{\max}$) of the domain, respectively.

2.3. *Velocity boundary conditions*

We impose a no-slip boundary condition on the velocity. Because the collision operator (the right-hand side of Equation (4)) is applied at the boundary the usual bounce-back condition is not appropriate as it would not ensure mass conservation [10].

Indeed after applying Equation (4) there are missing fields on the substrate sites because no fluid has been propagated from the solid. Missing fields are determined to fulfill the no-slip condition given by Equation (5) with $\mathbf{u} = 0$. This does not uniquely determine the f_i's. For most of the cases (i.e. 1–20) arbitrary choices guided by symmetry are used to close the system. This is no longer possible for sites 21–27 where four asymmetrical choices are available. Selecting one of those solutions or using a simple algorithm which chooses one of them at random each time step leads to very comparable and symmetrical results. Hence we argue that an asymmetrical choice can be used. See Reference [3] for a listing of the possible conditions.

The conservation of mass is ensured by setting a suitable rest field, f_0, equal to the difference between the density of the missing fields and the one of the fields entering the solid after collision.

3. WATER CAPTURE BY A DESERT BEETLE

As an example we consider the process by which a beetle species living in the Namib Desert collect drinking water on its back from a fog-laden wind [1].

The beetle's back is covered by tiny peaks of diameter 0.5 mm. The whole structure except the top of the peaks is coated in wax which forms a bumpy hydrophobic surface, whereas the top of the peaks are hydrophilic.

By tilting its body forwards into the wind, the beetle collects water from dense fog. The water condenses into droplets which settle at the top of the peaks. Once the droplets collected are large enough they spread beyond the peaks and may eventually coalesce with another neighbouring drop to form a larger drop. This drop is then heavy enough to roll downwards against the wind to reach the mouth of the beetle.

We demonstrate the ability of our model to deal with patterned substrates by considering a domain of size $L_x \times L_y \times L_z = 50 \times 50 \times 30$ covered by four $l_x \times l_y \times l_z = 10 \times 10 \times 5$ peaks. The minimum distance between the centers of the peaks is 20. The equilibrium contact angle is set to 70° on every surface site apart for those located at the top of the peaks where it is equal to 35°. The surface tension and the viscosity are tuned by choosing parameters $\kappa = 0.002$ and $\tau = 0.8$, respectively. The liquid density n_l and gas density n_g are set to $n_\mathrm{l} = 4.128$ and $n_\mathrm{g} = 2.913$ and the temperature $T = 0.4$. The system is initialized with a gas density greater than the equilibrium value ($n_\mathrm{g}^0 = 3.07$) and a body force $\mathbf{F} = (0, 0, -8e-8)$ is imposed to play the role of gravity.

We note that the density ratio of liquid and gas is unphysically small: this is necessary to achieve a stable simulation and must be taken into account when mapping onto physical time scales.

Simulation results are presented in Figure 2. Fluid initially condenses at the top of the peaks because of their hydrophilic nature. Due to the high water saturation, the droplets continue to spread beyond the hydrophilic area until coalescing to form a bumpy ring. Surface tension

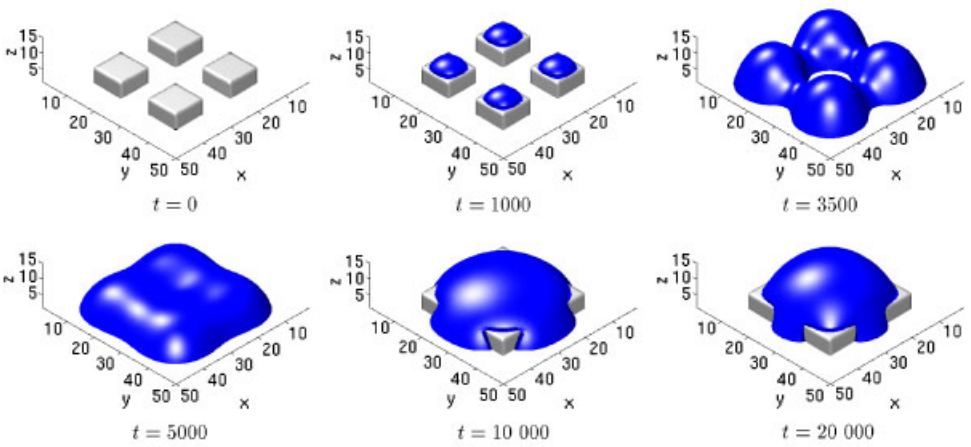

Figure 2. Fog condensing on a beetle's back. The top of the posts are hydrophilic, the remainder of the substrate is hydrophobic. t labels the time in simulation units.

forces the ring to shrink and eventually to form a single droplet which may be sufficiently large to roll into the wind to reach the beetle's mouth.

4. CONCLUSION

We have defined a lattice Boltzmann algorithm describing the spreading of a droplet on patterned substrates. As an example, we have used the model to reproduce the way a Namibian beetle captures water on its back from a fog-laden wind. Our simulation results are in qualitative agreement with the literature [1].

The chemical patterning on the beetle's back is essential to control the formation of the water droplets. It is less obvious why topological patterning has also evolved. Experiments have suggested the arrangements of the peaks is important in helping to guide the flow towards the beetle's mouth. The peaks might also slow down the wind velocity acting against the droplets. Moreover, the peaks might increase the contact angle of the hydrophobic region of the substrate [11] aiding the run-off. Further simulations are underway to investigate these questions.

ACKNOWLEDGEMENTS

We thank the Oxford Supercomputing Centre for providing supercomputing resources and A. Balazs for having drawn our attention to the Namibian beetle. AD acknowledges the support of the EC IMAGE-IN project GR1D-CT-2002-00663.

REFERENCES

1. Parler AR, Lawrence CR. Water capture by a desert beetle. *Nature* 2001; **414**:33–34.
2. Léopoldès J, Dupuis A, Bucknall DG, Yeomans JM. Jetting micron-scale droplets onto chemically heterogeneous surfaces. *Langmuir* 2003; **19**(23):9818–9822.

3. Dupuis A, Yeomans JM. Mesoscopic modelling of droplets on topologically patterned substrates. *ICCS04 Proceedings*, Lecture Notes in Computer Science, vol. 3039, 2004; 556–563, cond-mat/0401150.
4. Cahn JW. Critical point wetting. *Journal of Chemical Physics* 1977; **66**:3667–3672.
5. Succi S. *The Lattice Boltzmann Equation, for Fluid Dynamics and Beyond*. Oxford University Press: Oxford, 2001.
6. Swift MR, Orlandini E, Osborn WR, Yeomans JM. Lattice Boltzmann simulations of liquid–gas and binary fluid systems. *Physical Review E* 1996; **54**:5051–5052.
7. Dupuis A, Yeomans JM. Lattice Boltzmann modelling of droplets on chemically heterogeneous surfaces. *Future Generation Computer Systems* 2004; **20**:993.
8. Briant AJ, Wagner AJ, Yeomans JM. Lattice Boltzmann simulations of contact line motion. I. Liquid–gas systems. *Physical Review E* 2004; 031602.
9. Jacqmin D. Contact-line dynamics of a diffuse fluid interface. *Journal of Fluid Mechanics* 2000; **402**:57.
10. Chopard B, Dupuis A. A mass conserving boundary condition for lattice Boltzmann models. *International Journal of Modern Physics B* 2002; **17**:103–106.
11. Bico J, Marzolin C, Quéré D. Pearl drops. *European Physics Letters* 1999; **47**(2):220–226.

